ADVANCED TECHNOLOGIES AND MATERIALS VOL. 49, NO.2 (2024), 15 - 27
DOI: 10.24867/ATM-2024-2-002

1. Received: 10 September 2024
2. Revised: 01 October 2024
3. Accepted: 09 October 2024

Advanced Technologies & Materials
http://journal-atm.org
ISSN: 2620-0325 (print), ISSN: 2620-147X (online)

Influence of Infill Structure Shape and Density on the Mechanical Properties of FDM 3D-Printed PETG and PETG+CF Materials

Emine Hozdić,[a] *Elvis Hozdić,*[b]

[a]*Kranj School Centre, Kidričeva cesta 55, SI-4000, Kranj, Slovenia*
[b]*University of Novo mesto, Faculty of Mechanical Engineering, Na Loko 2, SI-8000, Novo mesto, Slovenia*

ABSTRACT

This paper investigates the impact of infill structure shape and density on the mechanical properties of Fused Deposition Modelling (FDM) 3D-printed materials, specifically PETG and PETG reinforced with carbon fibers (PETG+CF). The research aims to optimize additive manufacturing processes by examining how different infill geometries—hexagonal, triangular, and linear—and varying infill densities (30%, 60%, and 100%) influence the mechanical strength, tensile properties, and flexibility of the printed components. Experimental tensile tests were conducted on specimens to assess key mechanical parameters including maximum force, break force, Young's modulus, tensile strength, and nominal strain at break. Results indicate that infill shape and density significantly affect the mechanical performance of 3D-printed materials. Hexagonal infill structures demonstrated superior mechanical properties, with a 45.11% increase in maxi-mum force compared to triangular infill structures. Additionally, increasing the infill density from 30% to 100% resulted in a 69.13% increase in maximum force and a 64.87% increase in break force for PETG+CF specimens. These findings provide valuable insights for enhancing the quality and performance of FDM 3D-printed products, offering guidelines for the development of advanced materials with tailored mechanical properties for various industrial applications.

Key words: *Additive manufacturing, fused deposition modelling, infill structure, mechanical properties, PETG, PETG+CF*

1. INTRODUCTION

Additive manufacturing (AM), also known as 3D printing, has catalyzed transformative shifts in the creation and fabrication of diverse products. This technology builds three-dimensional objects by sequentially adding material in layers according to designs from computer-aided design (CAD) models. Over the past ten years, AM has seen substantial expansion and has become essential across multiple sectors, particularly in engineering and manufacturing. Its success is driven by its capacity for quick prototyping, its adaptability to various applications, and cost-efficiency, which have all significantly boosted its adoption [1]-[4]. There are various methods for classifying AM technologies. Some classifications are based on the type of material used for manufacturing (such as polymers, metals, ceramics, etc.), the material processing method during manufacturing (e.g., laser application, material extrusion technology), and the initial form of the material (liquid phase, wire form, powder form, etc.). Additionally, the complexity of classification is further compounded by the similarities among technologies in many aspects and the fact that the same technology can have multiple names. The American Society for Testing and Materials (ASTM) has classified additive manufacturing (AM) technologies into seven categories: (1) vat photopolymerization (VPP),

* *Corresponding author's.e-mail: elvis.hozdic@fs-unm.si*

(2) material Jetting (MJ), (3) powder bed fusion (PBF), (4) binder jetting (BJT), (5) directed energy deposition (DED), (6) sheet lamination (SHL), (7) material extrusion (MEX) [5].

Based on the classification provided by [1], AM can be divided into three primary categories depending on the base material used: solid-based, powder-based, and liquid-based technologies. Solid-based AM comprises several processes, such as laminated object manufacturing (LOM), fused deposition modeling (FDM), wire and arc additive manufacturing (WAAM), and electron beam freeform fabrication (EBF3). Powder-based AM involves techniques like selective laser sintering (SLS), electron beam melting (EBM), selective laser melting (SLM), and laser metal deposition (LMD). Lastly, liquid-based AM is mainly represented by material jetting (MJ) and vat photopolymerization (VPP).

AM technology enables the fabrication of intricate geometric structures with applications across various industries, including automotive, aerospace, biomedical, medical, construction, engineering sectors, and reverse engineering emphasizing exceptional material usage efficiency and production speed [6]-[10].

FDM is one of the methods of AM that is widely used due to its simplicity, efficiency, and accessibility [1], [11]-[13]. FDM operates on the principle of melt extrusion, which means it builds three-dimensional objects layer by layer by extruding melted thermoplastic material through a precisely controlled nozzle. The object is gradually shaped by extruding and depositing in layers onto a movable platform. This platform is maintained at a lower temperature so that the thermoplastic quickly solidifies. This process is relatively simple but is limited to thermoplastic materials and wax for precision casting. Key parameters, such as nozzle temperature, bed temperature, and layer height, directly affect the fractional behaviour of 3D-printed parts and shape the quality of the object.

In modern times, the materials used in AM processes significantly influence the development of these technologies. The selection of materials in AM processes brings specific properties that affect the strength, flexibility, thermal resistance, and aesthetic appearance of the final products. Understanding and choosing the right material is crucial for optimizing products tailored to specific applications.

FDM technology is suitable for a wide range of materials, including acrylonitrile butadiene styrene (ABS), acrylonitrile styrene acrylate (ASA), polyamide (PA), polylactide (PLA), and polyethylene terephthalate glycol-modified (PETG). Among the various materials used in FDM 3D printing, PLA and PETG have become popular due to their favourable mechanical properties and ease of use. To further enhance their performance, reinforcing additives such as carbon fibres (CFs) have been incorporated into these materials, resulting in composites with superior mechanical strength and stiffness [14].

PETG is a thermoplastic polyester material that offers a blend of exceptional mechanical properties, chemical resistance, and ease of use in AM. It is renowned for its high strength, durability, and impact resistance, making it suitable for a wide range of applications. PETG is often employed in the production of functional prototypes, mechanical parts, and end-use products. In terms of mechanical properties, PETG exhibits good tensile strength, enabling it to withstand significant loads and forces. Additionally, it boasts excellent impact resistance, which means it is highly resistant to cracking or breaking under sudden impacts or stresses. Its low shrinkage during printing ensures improved dimensional stability and minimal warping. Furthermore, PETG is noted for its high transparency and clarity, allowing for visually appealing printed objects [15]-[17].

PETG+CF is a composite material that combines the properties of PETG with CFs reinforcement. The addition of CFs enhances the mechanical properties, stiffness, and thermal stability of PETG. This composite material is particularly suitable for applications requiring high-performance characteristics. PETG+CF composites exhibit improved tensile strength and rigidity compared to pure PETG, while also maintaining excellent impact resistance. The thermal stability of PETG+CF composites is significantly enhanced, allowing them to withstand high temperatures without degradation [18], [19].

To ensure the proper sizing of parts made from given materials, it is essential to understand their mechanical properties. This knowledge is crucial to prevent unwanted deformations or even fractures under external loads. Consequently, the mechanical properties of materials elucidate the relationship between external loads and the resulting deformations. Key mechanical properties include strength (tensile, compressive, and bending), hardness, toughness, fatigue, creep, etc.

Numerous studies in the scientific community have assessed the mechanical behaviour of materials fabricated using FDM technologies of AM [20]-[35]. A comprehensive review of the literature suggests that research on the mechanical properties of 3D printed materials (including tensile, flexural, and torsional properties) branches into four primary areas. Initially, research centres on the influence of the characteristics of the input materials, such as their type and colour [20], [21]. Subsequent studies focus on how the design of the infill affects the mechanical properties [22], [23]. Another significant area of inquiry is the impact of various production process parameters, which include layer height, air gap, raster width, raster angle, build orientation, number of contours, floor/roof thickness, and deposition speed [24], [25]. Finally, research has also been conducted on how environmental conditions such as temperature, vibrations, and humidity affect the materials [14], [26].

Further examination of the literature [22], [23], [27]-[30] reveals the critical role of the infill structure, an essential component integrated into the interior of a 3D-printed product during its creation. Infill typically refers to the internal framework within the printed material of a product, which in traditional manufacturing would be solid. Common infill patterns include rectangular, triangular, linear, hexagonal (honeycomb), and diamond-shaped structures.

Infill usage in FDM-printed materials primarily offers benefits, such as reduced material use, lighter product weight, and quicker production times, which collectively lower the overall cost of the final product. Nonetheless, it is crucial to acknowledge that the infill structure significantly affects not only the mechanical properties but also other characteristics of the printed materials [22], [31]. In the paper [32], Chen et al. explored the impact strength and plasticity limit of various copolymeric materials, including PETG. Their findings indicated a notable reduction in the plasticity limit as the proportion of PCT within the copolymer increases. This inverse relationship highlights the potential trade-offs in material properties that must be considered when enhancing certain characteristics, such as impact resistance, by modifying the copolymer composition. This study adds important insights into the mechanical behaviour of PETG, suggesting that adjustments in PCT content could be critical for optimizing its performance for specific applications.

Srinivasan et al. [33] examined the influence of infill percentage on the tensile strength and surface roughness of materials. They discovered that a reduction in infill percentage by 80% resulted in a 45% decrease in tensile strength, while the surface roughness increased from 2.8 to 3.8 μm. Subsequently, researchers in the paper [34] investigated the impact of fill density and infill structure on the tensile strength and surface roughness of PETG products. Objects with 60% and 80% fill densities, structured with triangular and cubic infill patterns, were tested. The results demonstrated that specimens with a cubic infill structure achieved the highest tensile strength and the lowest surface roughness. In contrast, specimens with a triangular infill structure exhibited the lowest tensile strength and the highest surface roughness. Together, these findings illustrate how different fill settings and infill structures affect the mechanical properties and surface quality in FDM technology of AM.

In the paper [35], the authors examine the impact of FDM infill density on the mechanical properties of specimens printed with PETG and PETG+CF materials. Test specimens were printed with varying infill densities (25%, 50%,75%, and 100%), while other parameters remained constant. Infill density, followed by annealing, determines overall mechanical performance. Properties such as hardness, tensile strength, impact strength, and flexural strength improved with 100% infill density in PETG and PETG+CF samples. Enhanced interlayer diffusion bonding and mechanical properties were achieved through annealing, a secondary focus of this study. These findings offer valuable guidelines for producing functional parts using PETG+CF with 100% infill density and annealing, potentially replacing automotive and aeronautical structural components in the future.

The mechanical properties of PETG and PETG+CF materials printed using FDM technology are investigated in the paper [14]. In this paper, a hexagonal infill pattern with a density of 30% was used. The authors examined the effects of infill shape and density, as well as the impact of mineral engine oil, on the mechanical properties of FDM 3D-printed PETG and PETG+CF materials. PETG specimens exhibited intriguing behavior under oil exposure. The tensile strength decreased by 16.66% after seven days and by 16.85% after thirty days. Concurrently, there was a notable increase in the nominal strain at breaking—21.34% after seven days and 14.51% after thirty days—indicating that the material became more ductile over time. Additionally, the Young's modulus of PETG increased significantly, by 55.08% after seven days and 66.27% after thirty days, highlighting an increase in stiffness despite the overall reduction in tensile strength. For PETG+CF composites, the initial exposure to mineral engine oil resulted in slight increases in tensile strength (1.78%) and nominal strain at break (6.08%) after seven days. However, after thirty days, these samples experienced an 11.75% reduction in tensile strength. This suggests that while the initial exposure may temporarily enhance certain mechanical properties, prolonged exposure leads to degradation.

The aim of this study is to thoroughly investigate and analyze the impact of different infill structure designs and different infill density on the key mechanical parameters of FDM 3D-printed materials PETG and PETG+CF. From the perspective of developing a new generation of materials with optimal mechanical properties, this study examined two parameters: (1) the effect of infill structure shape (hexagon, triangle, and line) and (2) the infill density (30%, 60%, and 100%).

The main focus of the paper is on tensile strength and nominal strain at break, as these are crucial parameters that determine the usability and performance of 3D printed products. By analyzing the results, a more comprehensive understanding of how to adapt the infill structure design to meet the specific requirements of the final product will be gained. This contribution will help optimize the 3D printing process and achieve the desired mechanical properties of the products, which is essential for further advancements and innovations in this rapidly evolving field.

2. MATERIALS AND METHODS

2.1 Material specification

In this paper, two types of commercial materials were used: PETG and PETG+CF. The specifications and mechanical parameters of both materials are presented in Table 1 and Table 2, as provided by the manufacturer [36].

Table 1 – *PETG and PETG+CF filaments specifications* [36]

Material type	PETG	PETG+CF
Diameter (mm)	1.75	1.75
Color	green	black
Printing speed (mm/s)	60–90	60–90
Layer height (mm)	0.1–0.2	0.1–0.2
Extrusion temperature (°C)	240–250	230–250
Bed platform temperature (°C)	80–90	60–80

Table 2 displays mechanical parameters provided by the filament manufacturer [36] associated with test samples

that have a full infill density of 100%. The study utilized filaments with a circular cross-section, adhering to the specifications set by the manufacturer [36], which are defined by an average diameter of 1.75 mm and exhibit minimal variation in size.

Table 2 – *Mechanical properties of PETG and PETG+CF filaments* [36]

Material type	PETG	PETG+CF
Density (g/cm^3)	1.23	~1.28
Tensile strength (MPa)	40-45	40-43
Modulus of elasticity (MPa)	1000-1100	2100-2400
Elongation at break (%)	6.0-8.0	7.5-8.5
Heat deflection temperature (°C)	74	70

2.2 Preparation of specimens

The specimen model for conducting the experiment in this paper was designed in accordance with the ISO standard 527-2 [37] and prepared in the *SolidWorks 2020* software environment, see Fig. 1. After the design phase, the model was converted into STL format, which enables its use in software for generating *G-code*.
The STL file serves as the input for configuring and adjusting the parameters for the 3D-printing process.

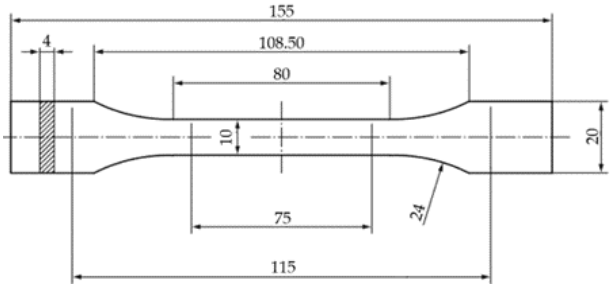

Fig. 1 *Design of the tensile test specimen following the guidelines of the ISO 527-2:2012 standard* [37]

2.3 Choosing the printer and setting process parameters

All the tensile test specimens were printed using the *Adventurer 4 Series 3D printer* by *FlashForge* [36].
The Adventurer 4 Series 3D printer features a touchscreen interface that facilitates intuitive navigation and delivers detailed status updates during the printing process. This interface allows for quick adjustments to critical parameters, including layer height, print speed, and temperature settings. Users can effortlessly refine these settings with a few taps or tweaks to enhance print quality and achieve the intended results.
The slicer *FlashPrint5* software enables adjusting printer parameters and managing and monitoring the print progress. Main printing parameters for both materials are presented in Table 3.
For each material, eighteen tensile test specimens were printed, totalling 36 specimens. All the specimens were created using 1000 g spools of PETG, and PETG+CF. The composite materials PETG+CF were prepared by the filament manufacturer [36].

Table 3 – *Main printing parameters*

3D Printing parameter	PETG	PETG+CF
Filament diameter (mm)	1.75	1.75
Infill pattern	Hexagon / Triangle / Line	Hexagon / Triangle / Line
Infill density (%)	30 / 60 / 100	30 / 60 / 100
Nozzle diameter (mm)	0.4	0.4
First layer maximum (mms^{-1})	10	10
Top solid layers	4	4
Bottom solid layers	3	3
Layer height (mm)	0.2	0.2
First layer height (mm)	0.3	0.3
Extrusion temperature (°C)	240	245
Bed temperature (°C)	90	80

2.4 Tensile testing

The input for the tensile testing is represented by the 3D-printed tensile test specimens. The testing procedure employed in this research is explained according to [37]. Tensile tests were performed using a Shimadzu AGS-X universal testing machine (Fig. 2) with a maximum load capacity of 10 kN and a testing speed of 6 mmmin^{-1}, in compliance with the ISO 527-2 standard.

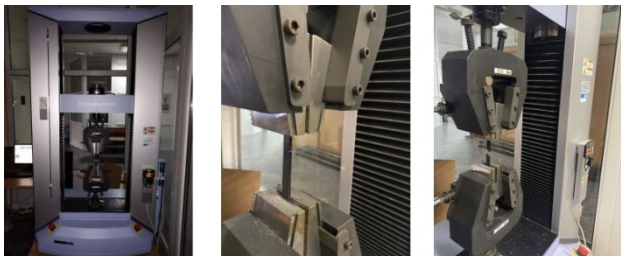

Fig. 2 *Tensile testing of 3D-printed specimens*

The Shimadzu Trapezium-X software facilitated the acquisition and monitoring of tensile test data. This robust software not only collects data such as Displacement (mm), Force (N), etc., for each test, but also generates force–displacement curves.
After collecting the tensile test data, the results were processed using Excel and are presented in the following section.

3. RESULTS AND DISCUSSION

3.1 Mechanical parameters of FDM 3D-printed PETG specimens with respect to the shape of the infill structure

The tested samples of FDM 3D-printed PETG material after the tensile test to determine mechanical properties with respect to infill structure shape are shown in Fig. 3.
The results of tensile tests for all tested samples of FDM 3D-printed PETG material, with respect to the infill structure shape, are presented in Table 4. The data in Table 4 is divided into three groups of samples:

a) 3D printed PETG material with a *hexagonal* infill structure shape and 30% infill density (PETG_411, PETG_412 and PETG_413) – Case 1,
b) 3D printed PETG material with a *triangular* infill structure shape and 30% infill density (PETG_421, PETG_422 and PETG_423) – Case 2,
c) 3D printed PETG material with a *line* infill structure shape and 30% infill density (PETG_431, PETG_432 and PETG_433) – Case 3.

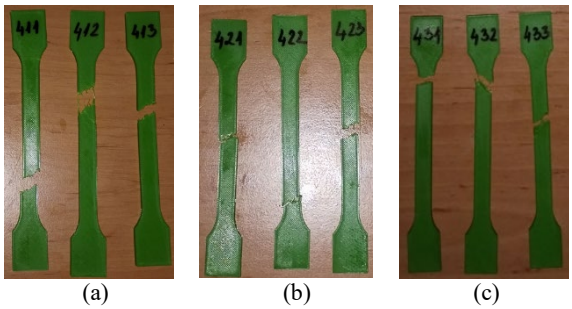

(a) (b) (c)

Fig. 3 *Specimens of FDM 3D printed PETG material after the tensile test: (a) hexagonal infill structure (Case 1); (b) triangular infill structure (Case 2); (c) line infill structure (Case 3). All specimens were printed with a 30% infill density*

The examination of data from tensile tests on specimens made with FDM 3D printing technology using PETG and various infill configurations (refer to Table 4) reveals significant variations in the behaviour of the material and in key measurable parameters. These parameters include the maximum force (F_{max}), force at break (F_{Break}), maximum displacement (ΔL), Young's modulus (E), tensile strength (σ), and nominal strain at break (ε). These findings are depicted in Fig. 4.

As illustrated in Fig. 4, the results for Case 1 were notably distinct from the other two cases, exhibiting the highest values in several critical mechanical properties, including maximum force, break force, and maximum displacement. This suggests that this case, with its hexagonal infill structure, possesses the superior mechanical properties among all the samples tested. Conversely, Case 2 demonstrated the poorest mechanical properties, as it registered the lowest values for maximum force, break force, and maximum displacement (Fig. 4). This indicates that this case was the least sturdy and tough among all the samples tested in this group.

Table 4 – *PETG specimens tensile test results, with respect to the infill structure shape*

Case	Specimen code	Max. Force (F_{max}) [N]	Break Force (F_{Break}) [N]	Max. Displacement (ΔL) [mm]	Young's modulus (E) [N/mm^2]	Tensile strength (σ) [N/mm^2]	Nominal Strain at Break (ε) [%]
Case 1	PETG_411	760.643	575.288	8.421	186.386	19.016	7.32
	PETG_412	753.291	553.561	9.910	184.023	18.832	8.61
	PETG_413	711.131	531.840	5.325	196.510	17.778	4.63
	Average	*741.688*	*553.564*	*7.885*	*196.510*	*18.542*	*6.85*
	St. Dev.	*26.718*	*30.722*	*2.339*	*6.633*	*0.668*	*2.03*
Case 2	PETG_421	555.841	398.366	3.915	227.688	13.896	3.40
	PETG_422	544.357	512.052	4.202	309.197	13.608	3.65
	PETG_423	597.787	460.347	4.901	117.483	14.944	4.26
	Average	*565.995*	*456.922*	*4.339*	*218.123*	*14.149*	*3.77*
	St. Dev.	*28.125*	*56.920*	*0.507*	*96.214*	*0.703*	*0.44*
Case 3	PETG_431	656.788	656.072	4.982	253.119	16.419	4.33
	PETG_432	683.745	282.613	5.901	270.229	17.093	5.13
	PETG_433	697.843	516.415	5.286	204.233	17.446	4.59
	Average	*679.459*	*485.033*	*5.390*	*242.527*	*16.986*	*4.68*
	St. Dev.	*20.860*	*188.697*	*0.468*	*34.249*	*0.522*	*0.41*

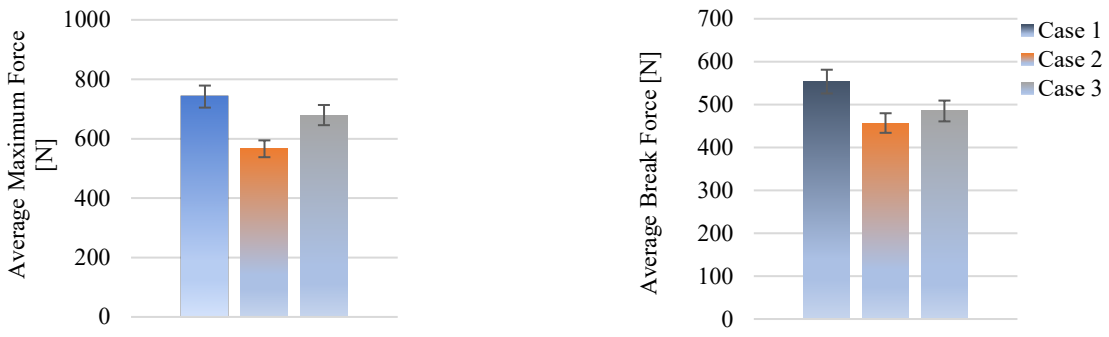

(a) (b)

Fig. 4 *Cont.*

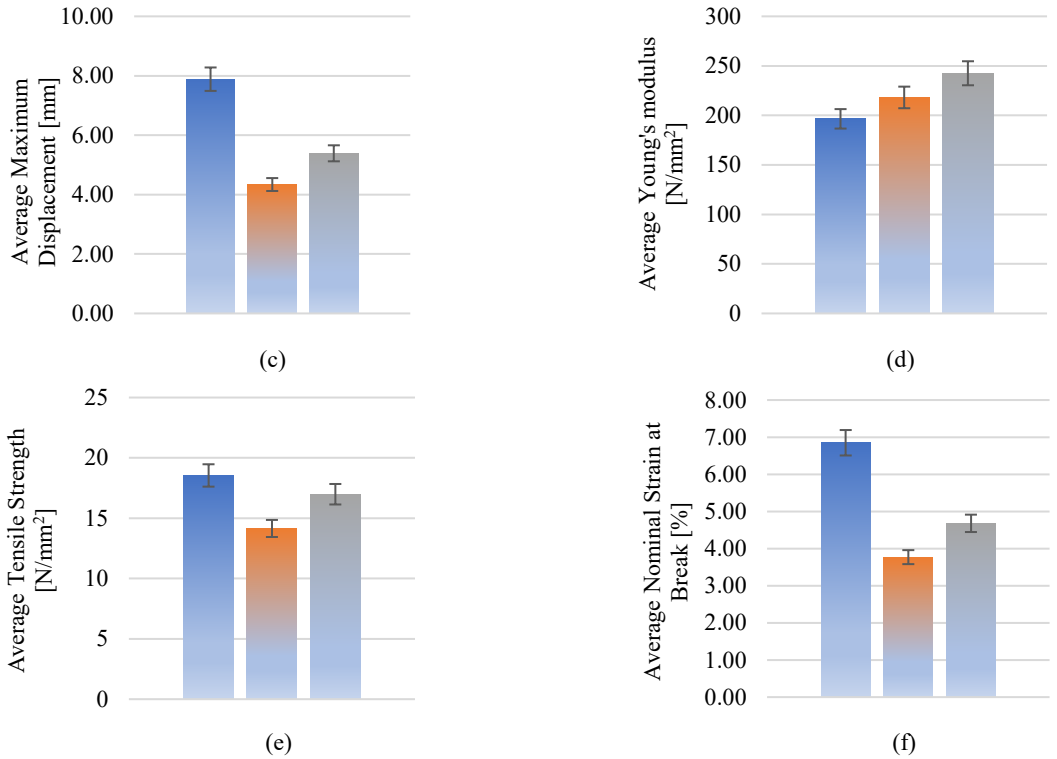

Fig. 4 *Graphic representation of average values of tensile test results of FDM 3D-printed PETG material specimens, based on the infill structure shape: (a) average maximum force; (b) average break force; (c) average maximum displacement; (d) average Young's modulus; (e) average tensile strength; (f) average nominal strain at break. All specimens were printed with a 30% infill density.*

Case 3 stood out with the highest value of the modulus of elasticity among the test subjects, as depicted in Fig. 4d. This indicates that this case is capable of withstanding substantial loads without permanent deformation and is highly rigid. Conversely, Case 1 displayed the lowest modulus of elasticity value (Fig. 4d), signifying that this sample is more susceptible to deformation under load and less rigid compared to the other cases.

Based on the data from Table 4 and Fig. 4, it is evident that Case 1 was distinguished among the other two cases, as it achieved the highest values in tensile stress and nominal strain at break. Notably, the nominal strain at break for Case 1 exceeded the values of Case 2 by 44.96% and Case 3 by 30.68%. This clearly demonstrates the exceptional performance and strength of Case 1 in comparison to the other two cases. On the other hand, Case 2 displayed the lowest values in tensile strength and nominal strain at break, indicating its relatively poor mechanical performance compared to the other two cases.

3.2 Mechanical parameters of FDM 3D-printed PETG+CF specimens with respect to the shape of the infill structure

The tested samples of FDM 3D-printed PETG+CF material after the tensile test to determine mechanical properties with respect to infill structure shape are shown in Fig. 5.

The results of tensile tests for all tested samples of FDM 3D-printed PETG+CF material, with respect to the infill structure shape, are presented in Table 5. The data in Table 5 is divided into three groups of samples:

a) 3D printed PETG+CF material with a *hexagonal* infill structure shape and 30% infill density (PETG+CF_711, PETG+CF_712 and PETG+CF_713) – Case 4,
b) 3D printed PETG+CF material with a *triangular* infill structure shape and 30% infill density (PETG+CF_721, PETG+CF_722 and PETG+CF_723) – Case 5,
c) 3D printed PETG+CF material with a *line* infill structure shape and 30% infill density (PETG+CF_731, PETG+CF_732 and PETG+CF_733) – Case 6.

(a) (b) (c)

Fig. 5 *Specimens of FDM 3D printed PETG+CF material after the tensile test: (a) hexagonal infill structure (Case 4); (b) triangular infill structure (Case 5); (c) line infill structure (Case 6). All specimens were printed with a 30% infill structure density.*

The examination of data from tensile tests on specimens made with FDM 3D printing technology using PETG+CF and various infill configurations (refer to Table 5) reveals significant variations in the behaviour of the material and in key measurable parameters. These findings are depicted in Fig. 6.

Based on the data presented in Fig. 6, it can be concluded that Case 6 was distinguished among the studied cases made of PETG+CF material. It exhibited a 5.56% higher tensile stress value compared to Case 5, indicating its greater strength. Furthermore, Case 6 had a 1.80% higher tensile strength value compared to Case 4, further emphasizing its performance under stress (Figure 8e).

On the other hand, Case 5 demonstrated the lowest value of tensile strength, which suggests its relatively inferior strength compared to the other two cases (Fig. 6e). Additionally, Case 6 showed the lowest value of nominal strain at break, indicating that it was less flexible compared to the other two cases. Case 4 was notable for its high value of nominal strain at break.

Table 5 – *PETG+CF specimens tensile test results, with respect to the infill structure shape*

Case	Specimen code	Max. Force (F_{max}) [N]	Break Force (F_{Break}) [N]	Max. Disp. (ΔL) [mm]	Young's modulus (E) [N/mm^2]	Tensile strength (σ) [N/mm^2]	Nominal Strain at Break (ε) [%]
Case 4	PETG+CF_711	826.375	726.660	5.223	327.756	20.659	4.54
	PETG+CF_712	809.439	517.633	6.258	188.796	20.235	5.44
	PETG+CF_713	805.489	521.827	6.301	169.598	20.137	5.47
	Average	*813.768*	*588.707*	*5.927*	*228.717*	*20.344*	*5.15*
	St. Dev.	*11.095*	*119.489*	*0.610*	*86.306*	*0.277*	*0.53*
Case 5	PETG+CF_721	796.032	573.625	4.955	265.200	19.900	4.30
	PETG+CF_722	787.966	499.535	5.005	191.641	19.699	4.35
	PETG+CF_723	721.137	647.720	7.405	211.311	18.028	6.43
	Average	*768.378*	*573.628*	*5.788*	*222.717*	*19.209*	*5.03*
	St. Dev.	*41.110*	*104.783*	*1.400*	*38.083*	*1.028*	*1.22*
Case 6	PETG+CF_731	703.351	616.654	4.415	313.116	17.583	3.83
	PETG+CF_732	844.375	751.448	4.991	234.759	21.109	4.34
	PETG+CF_733	850.121	621.986	5.362	223.862	21.253	4.66
	Average	*799.282*	*663.363*	*4.923*	*257.246*	*19.982*	*4.28*
	St. Dev.	*83.129*	*76.331*	*0.477*	*48.691*	*2.079*	*0.42*

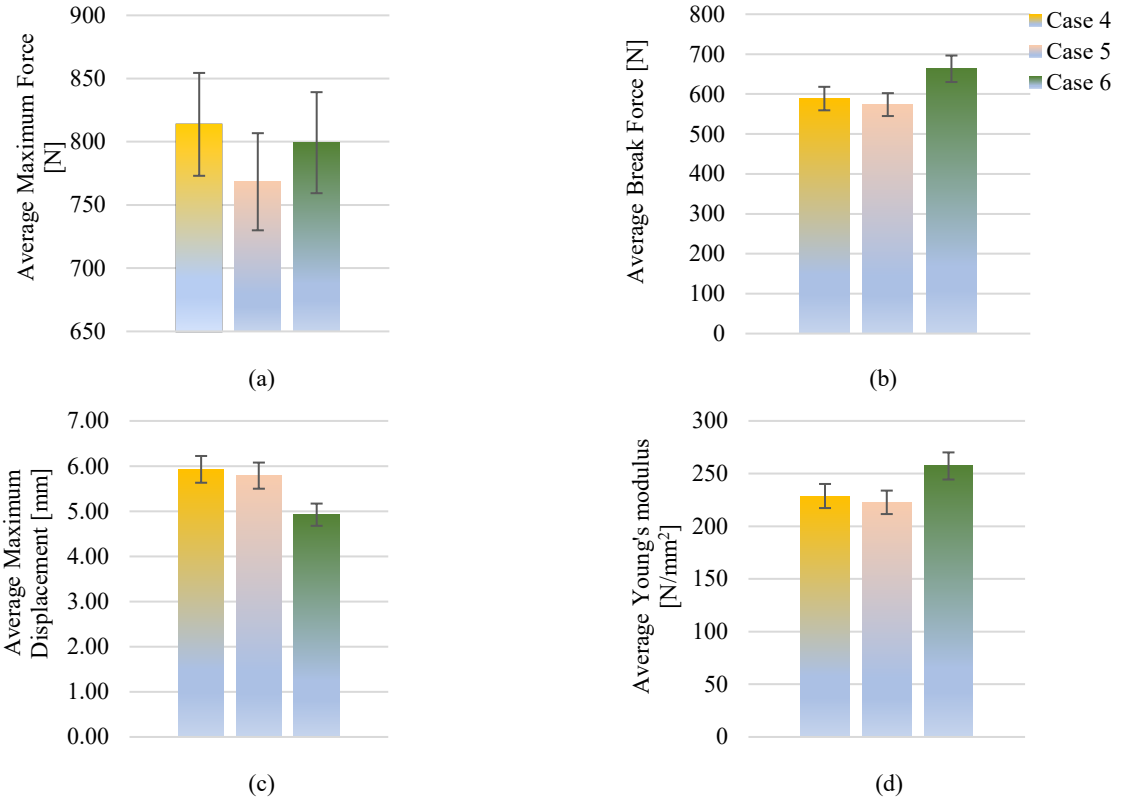

Fig. 6 *Cont.*

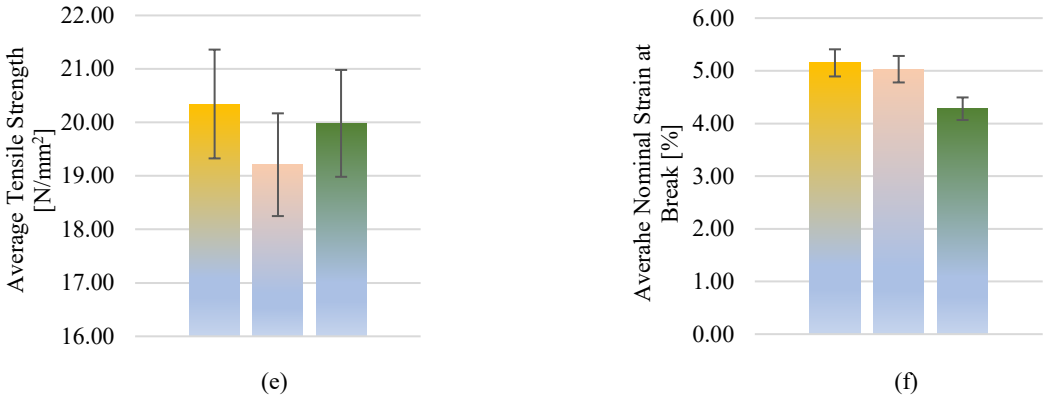

Fig. 6 *Graphic representation of average values of tensile test results of FDM 3D-printed PETG+CF material specimens, based on the infill structure shape: (a) average maximum force; (b) average break force; (c) average maximum displacement; (d) average Young's modulus; (e) average tensile strength; (f) average nominal strain at break. All specimens were printed with a 30% infill structure density.*

3.3 Mechanical parameters of FDM 3D-printed PETG specimens with different infill structure densities

The tested samples of 3D-printed PETG material after the tensile test to determine mechanical properties with respect to infill structure density are shown in Fig. 7.

(a) (b) (c)

Fig. 7 *Specimens of FDM 3D printed PETG material after the tensile test: (a) 30% infill structure density (Case 7); (b) 60% infill structure density (Case 8); (c) 100% infill structure density (Case 9). All specimens were printed with a line infill structure.*

The results of tensile tests for all tested specimens of FDM 3D-printed PETG material, with respect to the infill structure densities, are presented in Table 6. The data in Table 6 is divided into three groups of specimens:

a) 3D printed PETG material with a line infill structure shape and 30% infill structure density (PETG_431, PETG_432, and PETG_433) – Case 7,
b) 3D printed PETG material with a line infill structure shape and 60% infill structure density (PETG_434, PETG_435, and PETG_436) – Case 8,
c) 3D printed PETG material with a line infill structure shape and 100% infill structure density (PETG_437, PETG_438 and PETG_439) – Case 9.

Based on the data obtained from tensile testing of PETG material samples, where we varied the density of the line infill structure as detailed in Table 6, it has been created a graphical representation of these results. The interpreted results are presented in Fig. 8.

Table 6 – *PETG specimens tensile test results, with respect to the infill structure densities*

Case	Specimen code	Max. Force (F_{max}) [N]	Break Force (F_{Break}) [N]	Max. Displacement (ΔL) [mm]	Young's modulus (E) [N/mm²]	Tensile strength (σ) [N/mm²]	Nominal Strain at Break (ε) [%]
	PETG_431	656.788	656.072	4.982	253.119	16.419	4.33
Case 7	PETG_432	683.745	282.613	5.901	270.229	17.093	5.13
	PETG_433	697.843	516.415	5.286	204.233	17.446	4.59
	Average	*679.459*	*485.033*	*5.390*	*242.527*	*16.986*	*4.68*
	St. Dev.	*20.860*	*188.697*	*0.468*	*34.249*	*0.522*	*0.41*
	PETG_434	796.429	658.425	7.001	210.066	19.910	6.08
Case 8	PETG_435	792.003	607.435	7.892	342.788	19.800	6.86
	PETG_436	703.963	632.941	9.821	313.780	17.599	8.54
	Average	*764.132*	*632.930*	*7.446*	*288.878*	*19.103*	*7.16*
	St. Dev.	*52.155*	*36.055*	*1.441*	*69.777*	*1.304*	*1.26*
	PETG_437	1238.890	1020.690	8.867	328.558	30.972	7.71

Case 9	PETG_438	1258.410	1062.890	7.000	108.622	31.460	6.08
	PETG_439	1264.310	1102.670	6.320	161.634	31.607	5.49
	Average	*1253.870*	*1062.083*	*7.396*	*199.605*	*31.346*	*6.43*
	St. Dev.	*13.304*	*40.996*	*1.319*	*114.779*	*0.332*	*1.15*

The average maximum force value for Case 9 was 44.54% higher than that for Case 8 and 45.11% higher than that for Case 7 (Fig. 8a). Case 7 exhibited the lowest values in terms of maximum force, break force, and maximum displacement, indicating its inferior mechanical performance.

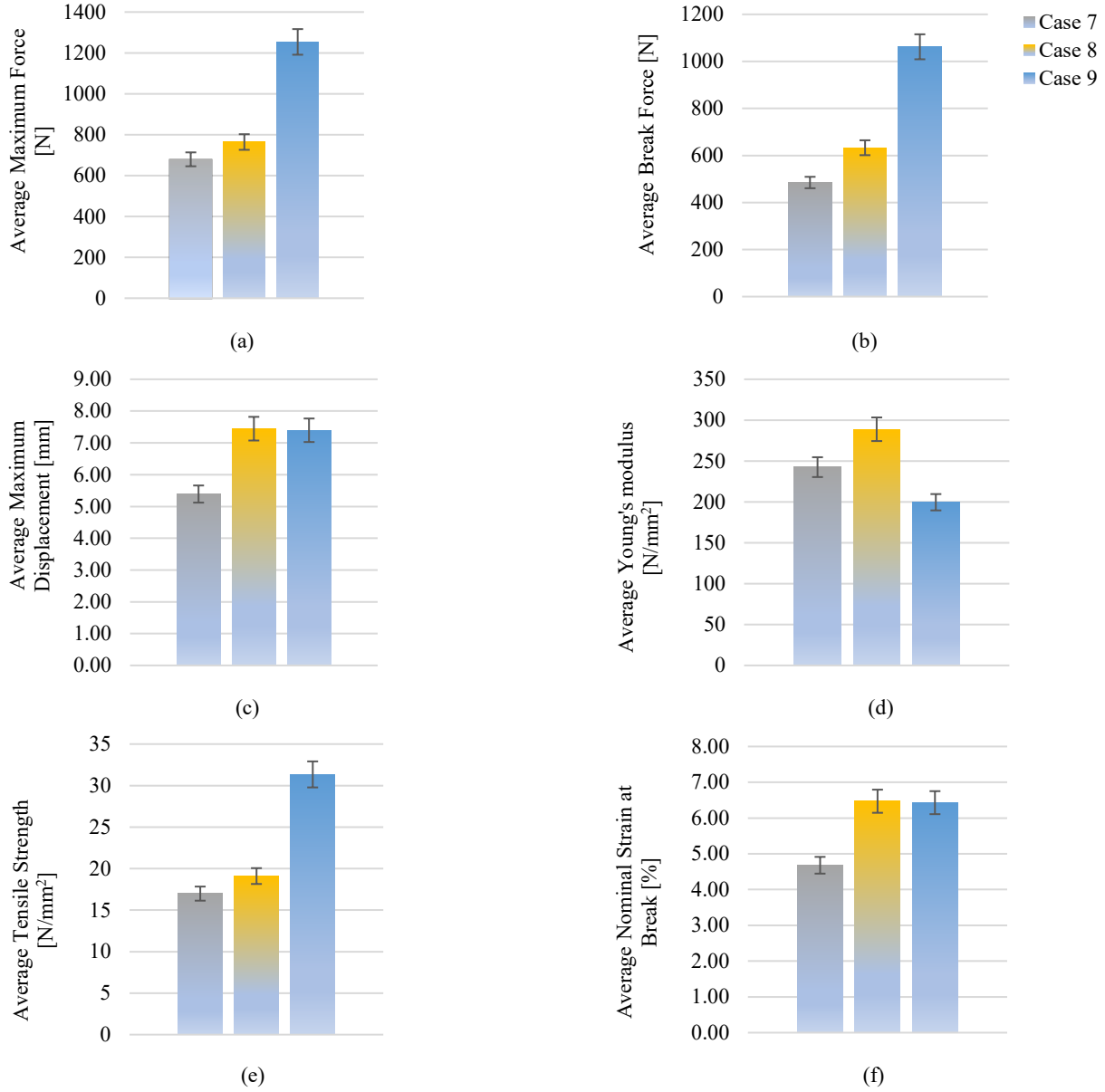

Fig. 8 *Graphic representation of average values of tensile test results of FDM 3D-printed PETG material specimens, based on the infill structure densities: (a) average maximum force; (b) average break force; (c) average maximum displacement; (d) average Young's modulus; (e) average tensile strength; (f) average nominal strain at break. All specimens were printed with the line infill structure.*

Case 8 stood out due to its highest values of elastic modulus (Young's modulus) and maximum displacement, indicating its ability to withstand loads without permanent deformation and its high strength. Interestingly, the maximum displacement between Cases 8 and 9 was minimal, suggesting similar behaviour of these two cases under various mechanical loads. Based on the data presented in Fig. 8, we can conclude that Case 7 exhibited the poorest mechanical properties among the PETG material cases, as it had the lowest tensile strength and

nominal strain at break. This indicates that Case 7 is less robust and performs worse under load compared to the other two cases. Case 9 proved to be the best in terms of tensile stress, achieving the highest value among all cases, demonstrating its exceptional mechanical strength. Conversely, Case 8 stood out for its highest nominal strain at break, meaning it has the greatest ability to stretch before breaking among all the cases. The results indicate varying mechanical properties for each case, with each having its own strengths and limitations regarding tensile strength and nominal strain at break.

3.4 Mechanical parameters of FDM 3D-printed PETG+CF specimens with different infill structure densities

The tested samples of 3D-printed PETG+CF material after the tensile test to determine mechanical properties with respect to infill structure density are shown in Fig. 9.

(a) (b) (c)

Fig. 9 *Specimens of FDM 3D printed PETG+CF material after the tensile test: (a) 30% infill structure density (Case 10); (b) 60% infill structure density (Case 11); (c) 100% infill structure density (Case 12). All specimens were printed with a line infill structure.*

The tensile test data for the 3D-printed PETG+CF material specimens, based on line infill structure density, are presented in Table 7. The data in Table 7 is divided into three groups of specimens:

a) 3D printed PETG+CF material with a line infill structure shape and 30% infill density (PETG+CF_731, PETG+CF_732, and PETG+CF_733) – Case 10,
b) 3D printed PETG+CF material with a line infill structure shape and 60% infill density (PETG+CF_734, PETG+CF_735, and PETG+CF_736) – Case 11,
c) 3D printed PETG+CF material with a line infill structure shape and 100% infill density (PETG+CF_737, PETG+CF_738, and PETG+CF_739) – Case 12.

A graphical representation of the average tensile test results for FDM 3D-printed PETG+CF specimens, based on the density of their line infill structure, is shown in Fig. 10.

Based on the data presented in Fig. 10, Case 12 stands out among these specimens, exhibiting the highest values for most recorded parameters, except for the elastic modulus (Young's modulus). The values for maximum force, break force, and maximum displacement for Case 12 were higher than those for Case 10, indicating its exceptional strength and durability. Additionally, Case 12 achieved a 69.13% higher maximum force compared to Case 10 (Fig. 10a) and a 64.87% higher value compared to Case 11, further confirming its superior performance.

In contrast, Case 10 exhibited the lowest values in the tensile test compared to the other two cases. This includes the lowest maximum force, indicating the relatively poor strength of this sample compared to Case 11 and Case 12.

Table 7 – *PETG+CF specimens tensile test results, with respect to the infill structure densities*

Case	Specimen code	Max. Force (F_{max}) [N]	Break Force (F_{Break}) [N]	Max. Displacement (ΔL) [mm]	Young's modulus (E) [N/mm^2]	Tensile strength (σ) [N/mm^2]	Nominal Strain at Break (ε) [%]
Case 10	PETG+CF_731	703.351	616.654	4.415	313.116	17.583	3.83
	PETG+CF_732	844.375	751.448	4.991	234.759	21.109	4.34
	PETG+CF_733	850.121	621.986	5.362	223.862	21.253	4.66
	Average	*799.282*	*663.363*	*4.923*	*257.246*	*19.982*	*4.28*
	St. Dev.	*83.129*	*76.331*	*0.477*	*48.691*	*2.079*	*0.42*
Case 11	PETG+CF_734	1.077.590	659.045	6.201	353.386	26.939	5.39
	PETG+CF_735	964.435	694.752	4.954	401.163	24.110	4.30
	PETG+CF_736	986.640	642.204	6.308	132.650	24.666	5.48
	Average	*1.009.555*	*665.334*	*5.821*	*295.733*	*25.238*	*5.06*
	St. Dev.	*15.701*	*26.833*	*0.753*	*143.240*	*1.499*	*0.66*
Case 12	PETG+CF_737	1544.31	1285.66	6.501	205.964	38.608	5.65
	PETG+CF_738	1566.21	1271.23	7.899	332.118	39.155	6.86
	PETG+CF_739	1557.91	1355.45	7.202	234.440	38.948	6.26
	Average	*1556.14*	*1.304.11*	*7.201*	*257.507*	*38.904*	*6.26*
	St. Dev.	*11.056*	*45.040*	*0.699*	*66.165*	*0.276*	*0.60*

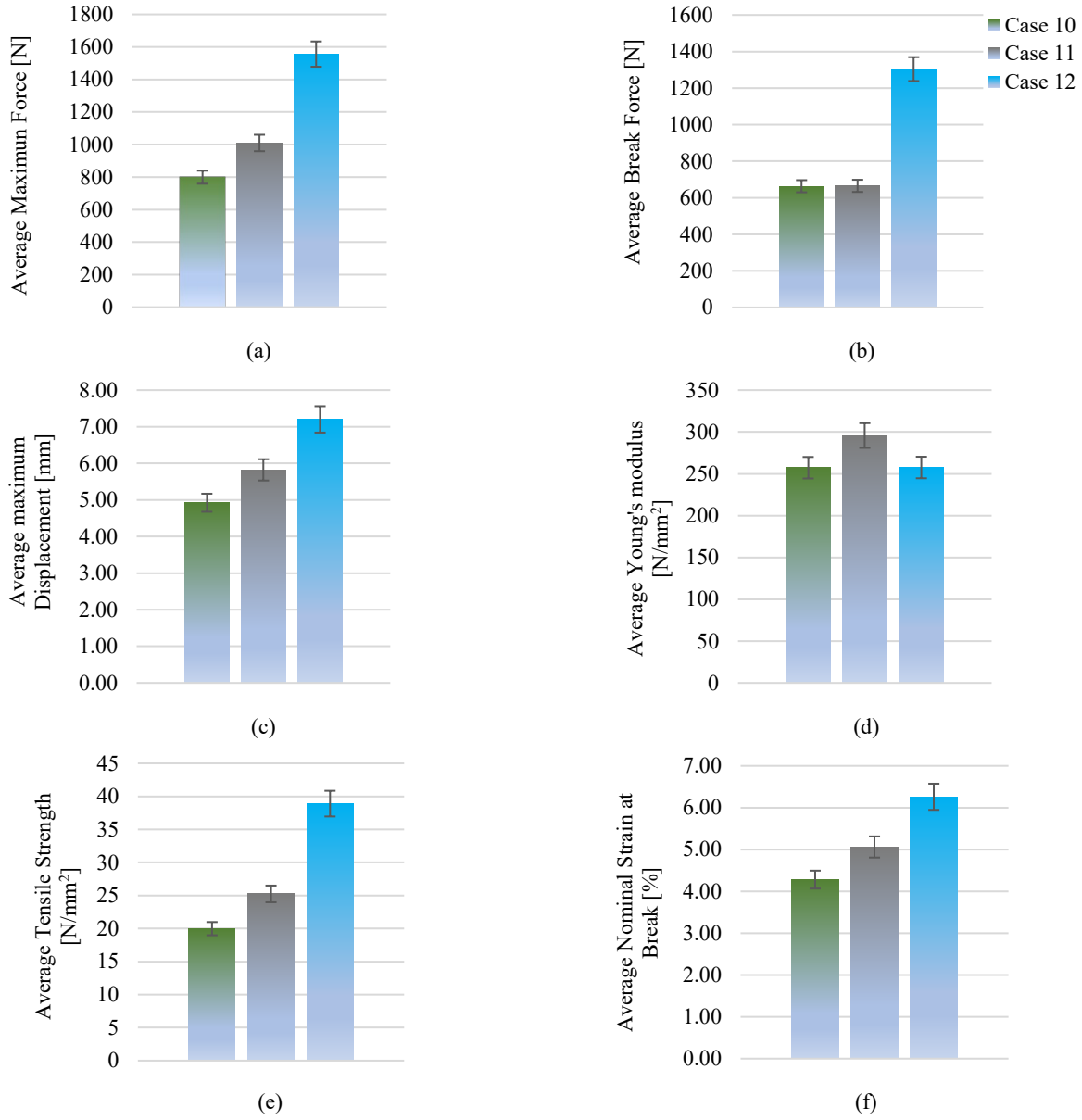

Fig. 10 *Graphic representation of average values of tensile test results of FDM 3D-printed PETG+CF material specimens, based on the infill structure densities: (a) average maximum force; (b) average break force; (c) average maximum displacement; (d) average Young's modulus; (e) average tensile strength; (f) average nominal strain at break. All specimens were printed with the line infill structure.*

3. CONCLUSIONS

Based on the comprehensive analysis of mechanical properties of FDM 3D-printed PETG and PETG+CF materials with varying infill structures and densities, several key conclusions can be drawn.

Firstly, regarding PETG materials, the tensile test results clearly indicate that the hexagonal infill structure (Case 1) consistently outperforms both triangular (Case 2) and linear (Case 3) structures in terms of maximum force, break force, and maximum displacement. This suggests that the hexagonal pattern provides superior mechanical strength and resilience under tensile stress compared to the other configurations. Conversely, the linear structure (Case 3) exhibits the highest Young's modulus, indicating its rigidity but lower ductility compared to the other patterns. In contrast, for PETG+CF materials, the hexagonal infill structure (Case 4) demonstrates the highest maximum force and displacement values, highlighting its enhanced toughness and ductility. Meanwhile, the triangular infill structure (Case 5) shows the lowest mechanical properties among the tested configurations, suggesting it is the least robust and flexible under load. Interestingly, the linear infill structure (Case 6) exhibits the highest Young's modulus, indicating it can withstand higher loads with minimal deformation compared to the other patterns.

Secondly, considering the influence of infill structure density on PETG materials, the results reveal that higher densities (60% and 100%) significantly enhance mechanical properties such as maximum force, break

force, and maximum displacement compared to lower densities (30%). This suggests that increasing infill density improves the overall strength and durability of FDM 3D-printed PETG components, making them more suitable for applications requiring higher mechanical performance.
Similarly, in PETG+CF materials, increasing infill density also enhances mechanical properties, with the 100% density (Case 12) showing the highest values for maximum force, break force, and maximum displacement. This indicates that higher densities improve the strength and toughness of PETG+CF components, making them suitable for demanding engineering applications.
Overall, these findings underscore the critical importance of infill structure design and density in optimizing the mechanical performance of FDM 3D-printed materials. By carefully selecting the appropriate infill pattern and density, manufacturers and designers can tailor the material properties to meet specific application requirements, ensuring enhanced performance and durability of FDM 3D-printed components in various industrial sectors. This study provides valuable insights for advancing the application of additive manufacturing technologies in engineering and manufacturing processes.

REFERENCES

[1] Gibson, I., Rosen, D.W., Stucker, B. and Khorasani, M.: Additive Manufacturing Technologies. Springer International Publishing, Cham, (2021)

[2] ISO 17296-2:2015, Additive Manufacturing-General Principles—Part 2: Overview of Process Categories and Feedstock. International Organization for Standardization, Geneva, Switzerland, (2015)

[3] Dave, H.K. and Patel, S.T.: Introduction to Fused Deposition Modelling Based 3D Printing Process. In *Fused Deposition Modeling Based 3D Printing. Materials Forming, Machining and Tribology*, Harshit, K., Dave, H.K., Davim J.P. (Eds.), Springer International Publishing, Cham, 1–21. (2021)

[4] Tofail, S.A.M., Koumoulos, E.P., Bandyopadhyay, A., Bose, S., O'Donoghue, L.M.T. and Charitidis, C.A.: Additive manufacturing: scientific and technological challenges, market uptake and opportunities, *Materials Today (21)*, 22–37, (2018)

[5] Goda, I. and Ganghoffer, J.-F.: 3D plastic collapse and brittle fracture models of trabecular bone from asymptotic homogenization method, *International Journal of Engineering Science (87)*, 58–82. (2015)

[6] Song, Y., Yan, Y., Zhang, R., Xu, D. and Wang, F.: Manufacture of the die of an automobile deck part based on rapid prototyping and rapid tooling technology, *Journal of Material Processing Technology (120)*, 237–242. (2002)

[7] Fereiduni, E., Ghasemi, A. and Elbestawi, M.: Selective Laser Melting of Aluminum and Titanium Matrix Composites: Recent Progress and Potential Applications in the Aerospace Industry, *Aerospace (7)*, 77. (2020)

[8] Wu, P., Wang, J. and Wang, X.: A critical review of the use of 3-D printing in the construction industry, *Automation in Construction (68)*, 21–31. (2016)

[9] Klocke, F. *et al.*: Turbomachinery component manufacture by application of electrochemical, electro-physical and photonic processes, *CIRP Annals (63)*, 703–726. (2014)

[10] Xu, J., Ding, L. and Love, P.E.D.: Digital reproduction of historical building ornamental components: From 3D scanning to 3D printing, *Automation in Construction (76)*, 85–96. (2017)

[11] Algarni, M. and Ghazali, S.: Comparative Study of the Sensitivity of PLA, ABS, PEEK, and PETG's Mechanical Properties to FDM Printing Process Parameters, *Crystals (11)*, 995. (2021)

[12] Naveed, N.: Investigating the Material Properties and Microstructural Changes of Fused Filament Fabricated PLA and Tough-PLA Parts, *Polymers (13)*, 1487. (2021)

[13] Zhang, P., Wang, Z., Li, J., Li, X. and Cheng, L.: From materials to devices using fused deposition modelling: A state-of-art review, *Nanotechnology Review (9)*, 1594–1609. (2020)

[14] Hozdić, E. and Hozdić, E.: Comparative Analysis of the Influence of Mineral Engine Oil on the Mechanical Parameters of FDM 3D-Printed PLA, PLA+CF, PETG, and PETG+CF Materials, *Materials (16)*, 6342. (2023)

[15] Dolzyk, G. and Jung, S. Tensile and Fatigue Analysis of 3D-Printed Polyethylene Terephthalate Glycol, *Journal of Failure Analysis and Prevention (19)*, 511–518. (2019)

[16] Teraiya, S., Vyavahare, S. and Kumar, S.: Experimental Investigation on Influence of Process Parameters on Mechanical Properties of PETG Parts Made by Fused Deposition Modelling. In *Advances in Manufacturing Processes. Lecture Notes in Mechanical Engineering*, Dave, H.K., Nedelcu, D. (Eds,), Springer, Singapore, 283–293. (2021)

[17] Srinivasan, R. *et al.*: Effect on infill density on mechanical properties of PETG part fabricated by fused deposition modelling, *Material Todays: Proceedings (27)*, 1838–1842. (2020)

[18] Kasmi, S., Ginoux, G., Allaoui, S. and Alix, S.: Investigation of 3D printing strategy on the mechanical performance of coextruded continuous carbon fiber reinforced PETG, *Journal of Applied Polymer Science (138)*, 1–26. (2021)

[19] Kumar, K.S., Soundararajan, R., Shanthosh, G., Saravanakumar, P. and Ratteesh, M.: Augmenting effect of infill density and annealing on mechanical properties of PETG and CFPETG composites fabricated by FDM, *Materials Today: Proceedings (45),* 2186–2191. (2021)

[20] Hodžić, D., Pandžić, A., Hajro, I. and Tasić, P.: Strength comparison of FDM 3D printed PLA made by different manufacturers, *TEM Journal (9)*, 966–970. (2020)

[21] Wittbrodt, B. and Pearce, J.M.: The effects of PLA colour on material properties of 3-D printed

components, *Additive Manufacturing (8)*, 110–116. (2015)
[22] Bakır, A.A., Neshani, R. and Özerinç, S.: Mechanical Properties of 3D-Printed Elastomers Produced by Fused Deposition Modeling. In *Fused Deposition Modeling Based 3D Printing. Materials Forming, Machining and Tribology,* Dave, H.K. and Davim, J.P. (Eds.*)*, Springer, Cham. (2021)
[23] Dave, H.K., Patadiya, N.H., Prajapati, A.R. and Rajpurohit, S.R.: Effect of infill pattern and infill density at varying part orientation on tensile properties of fused deposition modeling-printed poly-lactic acid part, *Proceedings of the Institution of Mechanical Engineers, Part C: Journal of Mechanical Engineering Science (235/10)*, 1811–1827. (2021)
[24] Abeykoon, C., Sri-Amphorn, P. and Fernando, A.: Optimization of fused deposition modeling parameters for improved PLA and ABS 3D printed structures, *International Journal of Lightweight Materials and Manufacture (3)*, 284–297. (2020)
[25] Popescu, D., Zapciu, A., Amza, C., Baciu, F. and Marinescu, R.: FDM process parameters influence over the mechanical properties of polymer specimens: A review, *Polymer Testing (69)*, 157–166. (2018)
[26] Moetazedian, A., Gleadall, A., Han, X. and Silberschmidt, V.V.: Effect of environment on mechanical properties of 3D printed polylactide for biomedical applications, *Journal of the Mechanical Behavior of Biomedical Materials (102)*, 103510. (2020)
[27] Bergonzi, L., Vettori, M., Stefanini, L. and D'Alcamo, L.: Different infill geometry influence on mechanical properties of FDM produced PLA, *IOP Conference Series: Materials Science and Engineering (1038/1)*, 012071. The 49th AIAS Conference (AIAS 2020), Genova, Italy. (2021)
[28] Khan, S.A., Siddiqui, B.A., Fahad, M. and Khan, M.A.: Evaluation of the Effect of Infill Pattern on Mechanical Strength of Additively Manufactured Specimen. In *Materials Science Forum*, Trans tech Publications *(887),* 128-132. (2017)
[29] Dudek, P.: FDM 3D printing technology in manufacturing composite elements, *Archives of Metallurgy and Materials (58/4)*, 1415-1418. (2013)
[30] Chiulan, I., Frone, A.N., Brandabur, C. and Panaitescu, D.M.: Recent Advances in 3D Printing of Aliphatic Polyesters, *Bioengineering (5)*, 1-18, (2017)
[31] Dezaki, M.L. and Ariffin M.K.A.M.: The Effects of Combined Infill Patterns on Mechanical Properties in FDM Process, *Polymers (12)*, 2792. (2020)
[32] Chen, L.P., Yee, A.F. and Moskala, E.J.: The Molecular Basis for the Relationship between the Secondary Relaxation and Mechanical Properties of a Series of Polyester Copolymer Glasses, *Macromolecules (32)*, 5944–5955. (1999)
[33] Srinivasan, R., Ruban, W., Deepanraj, A., Bhuvanesh, R. and Bhuvanesh, T.: Effect on infill density on mechanical properties of PETG part fabricated by fused deposition modelling, *Materials Today: Proceedings (27)*, 1838–1842. (2020)
[34] Srinivasan, R., Prathap, P., Raj, A., Kannan, S.A. and Deepak, V.: Influence of fused deposition modeling process parameters on the mechanical properties of PETG parts, *Materials Today: Proceedings (27)*, 1877–1883. (2020)
[35] Kumar, K.S., Soundararajan, R., Shanthosh, G., Saravanakumar, P. and Ratteesh, M.: Augmenting effect of infill density and annealing on mechanical properties of PETG and CFPETG composites fabricated by FDM, *Materials Today: Proceedings (45)*, 2186–2191. (2021)
[36] FLASHFORGE, *Comparison between FlashForge PLA, PLA Pro, PLA-CF, ABS, ABS Pro, PETG, PETG Pro, PETG-CF*. [Online]. Available: https://www.flashforge.com/news-detail/which-3d-printer-materials-to-use-for-printing (accessed on 18 August 2023).
[37] ISO 527-2: 2012: *Plastics—Determination of Tensile Properties—Part 2: Test Conditions for Moulding and Extrusion Plastics*. International Organization for Standardization, Geneva, Switzerland. (2012)

NOTE

This paper is based on the papers presented at 15th International Scientific Conference MMA 2024 – Flexible Technologies, organized by University of Novi Sad, Faculty of Technical Sciences, 24 - 26. September 2024, Novi Sad, Serbia.